Chemical Engineering Journal 499 (2024) 156238

Contents lists available at ScienceDirect

Chemical Engineering Journal

journal homepage: www.elsevier.com/locate/cej

Effect of moisture (2 mol%) on CO_2 enhanced desorption from nano-dispersed Na_2O/Al_2O_3 for direct air capture

Soosan Kim, Xiao Lin, Robert J. Farrauto *

Department of Earth and Environmental Engineering, Columbia University in the City of New York, 500 West 120th Street, New York, NY 10027, USA

ARTICLE INFO

Keywords:
Direct air capture
CO_2 capture
"Na_2O"/γ-Al_2O_3
2 mol % moisture
Enhanced desorption
Multiple cycle aging tests

ABSTRACT

This study demonstrates enhanced CO_2 desorption from nano-dispersed "Na_2O"/γ-Al_2O_3 using a low moisture content purge gas. As little as 2 mol% moisture (generated at the vapor pressure of water at 20 °C) present in an inert purge gas enhances the amount and rate of CO_2 desorbed over a series of temperatures relative to a dry purge. Multi-cycle aging tests of 317 h, at various desorption conditions, confirmed the stability of system efficiency with the potential for energy savings in avoiding steam production commonly used for CO_2 desorption.

1. Introduction

The ever-increasing carbon dioxide (CO_2) concentration in the atmosphere, reaching ~ 423 ppm in 2024, is recognized as a significant contributor to climate change. Thus, direct air capture is essential to reduce the CO_2 levels to pre-industrial revolution values of 280 ppm [1]. In parallel, increases in CO_2 during the green transition must be minimized [2] using fossil-free renewable energy.

Direct air capture (DAC) technology has developed in various ways, including not only the use of specialized high-capacity amines [3] but also ion exchange liquids [4], electrochemical processes [5], and membranes [6]. The cost for DAC is high primarily due to energy-intensive processes of separating captured CO_2 from the saturated amine in the aqueous solutions[7]. According to the World Resources Institute, the reported range of costs for DAC varies between $250 and $600 per ton of CO_2 [8]. A large-scale facility in Iceland by Climeworks (Mammoth) suggests $600 per ton of CO_2 for DAC [9]. Any improvement in decreasing process energy costs would be an important contribution to mitigating climate change with lower energy consumption [10]. The technology discussed in this paper shows an initial feasibility study that may be a step toward achieving this goal.

CO_2 capture using aqueous amine scrubbing from flue gases was developed as a source for CO_2 in urea production as early as 1930 [11]. Today, it is considered the "state of the art" for CO_2 capture due to its high level of adsorption capacity, rates, selectivity, and separation from the aqueous amine by distillation [12]. Steam is also considered to improve CO_2 separation from solid sorbents for temperature vacuum swing adsorption/desorption cycles [13]. Also, catalytic materials, such as SnO_2-modified attapulgite (SnO2/ATP), were used to increase CO_2 desorption rates and reduce heat energy input [14]. The major challenges of CO_2 capture include the need for large-scale infrastructure [15] and its energy-intensive nature, especially for regeneration [16].

Solid inorganic sorbents are considered one of many alternative capture technologies offering the advantages of corrosion-free operations and high stability relative to organic amines [17]. Recently, specific inorganic solid sorbents have been shown to have excellent selectivity for CO_2 while providing stability over an extended period of cyclic aging in simulated ambient air (400 ppm CO_2 in moisture-containing air). However, separating the captured CO_2 from the sorbent still requires excessive energy [18].

Na_2CO_3 is a representative CO_2 adsorbent with high sorption capacity under humid conditions [19]. The key reaction with moisture is believed to be some variation of the formation of alkaline sodium bicarbonate:

$$Na_2CO_3 + H_2O + CO_2 \leftrightarrow 2NaHCO_3$$

Nano-dispersed alkali have strong basic chemistry on high surface area carriers such as Al2O3, thereby possessing increased CO_2 adsorption capacity [20]. For example, Goldman reported that a sorbent for DAC containing 10 % sodium oxide (speculated to be "Na_2O") dispersed on Al_2O_3 washcoated onto a ceramic monolith, demonstrating stable CO_2 capture and desorption for hundreds of hours under simulated

* Corresponding author.
E-mail address: RF2182@columbia.edu (R.J. Farrauto).

https://doi.org/10.1016/j.cej.2024.156238
Received 11 August 2024; Received in revised form 25 September 2024; Accepted 26 September 2024
Available online 27 September 2024

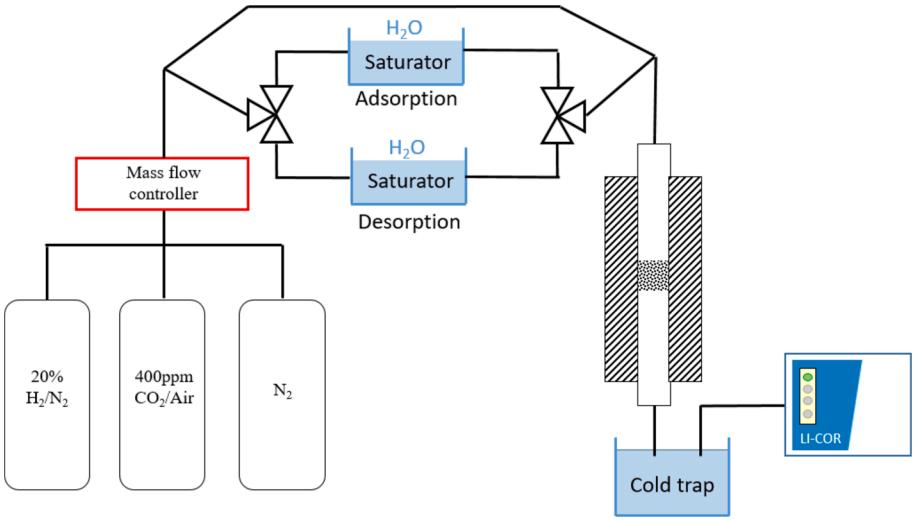

Fig. 1. Schematic of the reactor system.

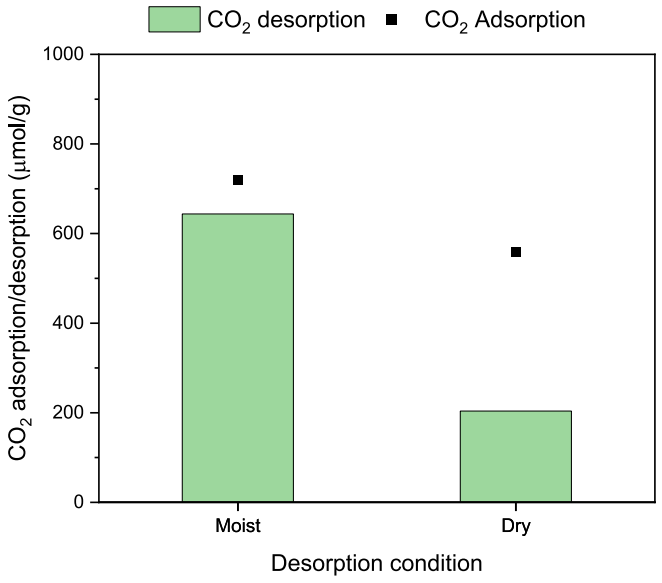

Fig. 2. The adsorption (black squares) and desorption performance of samples, with 0.25 %Ru, 10 % "Na_2O"/Al_2O_3 under both moist (left) and dry desorption (right) conditions. Adsorptions were always conducted with a gas flow at 20 °C with 400 ppm CO_2/air + 2 mol% H_2O, while temperature-swing desorption was conducted in N_2 from room temperature to 150 °C with 5 °C/min heating rate (moist: N_2 + 2 mol% H_2O, dry: pure N_2). Each data point is an average of 5 repeated runs.

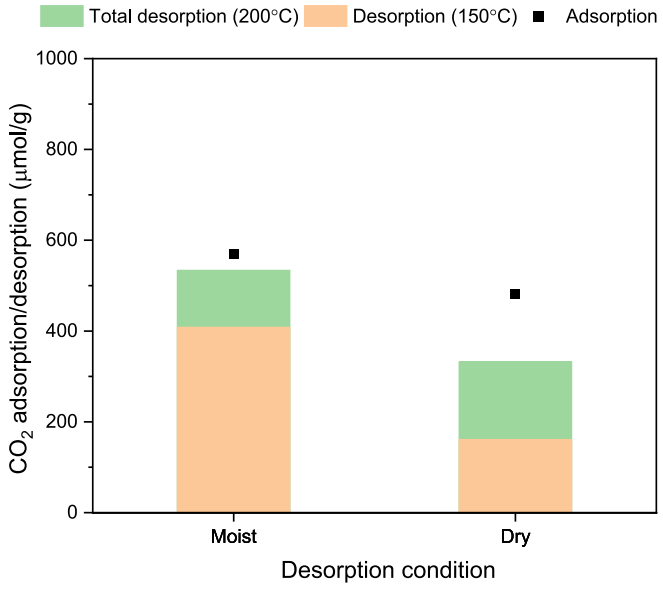

Fig. 3. All adsorptions were conducted in humid conditions. Desorption performance is shown in the sample of 1.0 % Ni, 10 % "Na_2O"/Al_2O_3 with moist (left) and dry desorption (right). The adsorption was conducted with a gas flow at 20 °C with 400 ppm CO_2/air + 2 mol% H_2O, and the temperature-swing desorption was conducted from room temperature to 150 °C then to 200 °C with 5 °C /min heating rate (moist: N_2 + 2 mol% H_2O, dry: pure N_2).

ambient air cyclic conditions followed by dry desorption up to 200 °C. Additionally, he reported a significant enhancement of CO_2 adsorption capacity in the presence of moisture at room temperatures, speculated to be due to the formation of nano-dispersed $NaHCO_3$ [21]. This finding is confirmed in several other publications using similar materials [22–24].

This paper demonstrates that CO_2 captured with "Na_2O"/-Al_2O_3 shows enhanced desorption capacity and rates when using moisture generated at low temperatures (2 mol%) in the purge gas. This avoids the need for energy-intensive steam generation.

2. Material/experimental

2.1. Sample preparation

Sorbent materials were prepared using previously published methods [21]. An aqueous solution of sodium carbonate (Na_2CO_3) was impregnated into 300 μm γ-Al_2O_3 granules (Sasol TH100) using the incipient wetness method. Multiple impregnation steps were needed to reach the target loading (10 % "Na_2O"). Between each step, the sample was dried at 120 °C for 4 h in static air. When the sorbent was fully loaded, it was calcined at 400 °C for 4 h in static air.

A catalytic metal is optionally included in the preparation to increase the extent of the Na_2CO_3catalytic hydrogenation, which significantly enhances CO_2 adsorption [26]. To incorporate Ru into the sorbent, an aqueous solution of ruthenium nitrosyl nitrate ($Ru(NO)(NO_3)_3$) precursor salt (Alfa Aesar, containing 32 % Ru) was impregnated to achieve a loading of 0.25 % Ru. Nickel nitrate hexahydrate ($Ni(NO_3)_2 \bullet 6H_2O$) salt (Sigma Aldrich, Ni 99.9 %) was used as a possible substitute for Ru since Ni metal is also capable of decomposing Na_2CO_3 during the H_2 pretreatment. Either salt in deionized water was added dropwise to the

Table 1
The amount of adsorbed and desorbed CO_2 using 1.0 % Ni, 10 % "Na_2O"/Al_2O_3. Adsorption was conducted at ambient conditions with 2 mol % H_2O and a flow rate of 400 ml/min air containing 400 ppm CO_2. Desorption was conducted at two temperatures (150 °C and 200 °C) under moist (100 ml/min N_2, and 2 mol% H_2O) and dry (100 ml/min N_2) conditions. Each data is an average of 3 cycles with a percent error.

Unit (**μmol**/**g**)	Steady state (2 mol% H_2O)	Temperature	
		150 °C	200 °C
Ambient Adsorption after des 200 °C	567 (± 0.4 %)		
Moist Desorption		390 (± 3.7 %)	528 (± 0.9 %)
Ambient Adsorption after des 200 °C	491 (± 1.6 %)		
Dry desorption		158 (± 1.7 %)	330 (± 0.7 %)

Table 2
Adsorption, purge, and desorption capabilities of 2.5 % Ni, 10 % "Na_2O"/Al_2O_3 at three different desorption temperatures under moist conditions (100 ml/min N_2, 5 °C /min, and 2 mol% H_2O in N_2). All adsorptions were conducted at 20 °C with 2 mol % H_2O in air.

Unit(**μmol**/**g**)	Temperature		
	120 °C	150 °C	200 °C
Ambient Adsorption (2 mol% H_2O)	309	416	659
Moist Desorption	220	337	572

pre-calcinated sample. The final loading was either 0.25 % Ru or 1 %/2.5 % Ni when dried at 120 °C for 4 h in static air. It is imperative to avoid extensive oxidation of the Ni since it must be in its reduced state to catalytically hydrogenate the Na_2CO_3 to "Na_2O". The sample is fixed in the reactor and subjected to flowing 20 % H_2/N_2 for pretreatment at 350 °C for 20 h with a temperature ramp of 5 °C/min. CH_4 is measured during the pretreatment to confirm the catalytically hydrogenation of the dispersed Na_2CO_3. The final material comprises 0.25 % Ru or 1 %/2.5 % Ni, intimately dispersed on 10 % "Na_2O"/Al_2O_3 granules.

2.2. Reactor

2.2.1. Setup

All direct air capture and desorption procedures were conducted using the reactor schematic shown in Fig. 1. Three cylinders (100 % N_2, 20 % H_2/N_2, and 400 ppm CO_2 + air) were connected to three discrete mass flow meters (MSK instrument) with a three-way valve, establishing the desired gas flow path. This arrangement allows gas flows for adsorption in simulated air with ambient humidity and desorption in N_2 under either moist or dry conditions. Two separate saturators were used since the water in the adsorption feed gas path becomes saturated with CO_2, which could affect desorption results if only a single path were utilized. Gas flows through the water saturator for both moist adsorption and moist desorption generated at 20 °C, resulting in about 2 mol% moisture. It should be noted that the humidity will decrease during temperature-swing desorption, but the gas still contains 2 mol% moisture. All adsorption steps were conducted at 20 °C with 2 mol% moisture and a flow of 400 ml/min simulated air containing 400 ppm CO_2. Any moisture in the exit gases was condensed in the cold trap before entering the CO_2/H_2O analyzer (Li-Cor 850).

The reactor quartz tube (O.D. = 12.75 mm, I.D = 10.5 mm, L = 500 mm) was located within a Mellon Microthermal Furnace (USA) with a temperature controller. The sample thermocouple (K-type Omega, USA) was positioned at the inlet center of the sample bed supported by glass wool (Supelco, USA); The void volume in the reactor tube was filled with glass beads (4 mm McKesson, USA) to reduce the dead volume for more rapid analysis.

2.2.2. Sequence procedure of adsorption and desorption

All samples were pretreated in the reactor by the procedure stated in Section 2.1. Cyclic adsorption and desorption for the granular sorbent particles were tested following the steps listed below.

1) Capture stage: A flow rate of 400 ml/min of air containing 400 ppm CO_2 passes through the water saturator at 20 °C, resulting in about 2 mol% moisture. The 2 mol% moisture refers to absolute humidity, and the partial pressure calculation is shown below in yellow highlight (P_{H2O} (20 °C) refers to the partial pressure of water at 20 °C, and P_{atm} refers to the atmospheric pressure):

$$Mol\%Moistureinair(20^{\circ}C) = \frac{P_{H_2O}(20^{\circ}C)}{P_{atm}} = \frac{17.5\ mmHg}{760\ mmHg} \approx 2mol\% \quad (1)$$

2) Purge stage: The reactor is then purged with dry N_2 at 100 ml/min for 20 min to remove residual feed gas until no CO_2 is observed in the exit gas.

3) Desorption stage: A flow of N_2 (100 ml/min) is passed through the other saturator, generating about 2 mol% moisture. Simultaneously, the furnace is heated at 5 °C/min to the various maximum desorption temperatures, as indicated in the figures, until the CO_2 level decreases to a baseline value.

2.2.3. Characterization

A Panalytical Xpert3 Powder XRD was used. The X-ray diffraction (XRD) device was outfitted with copper K-alpha XRD. Patterns were

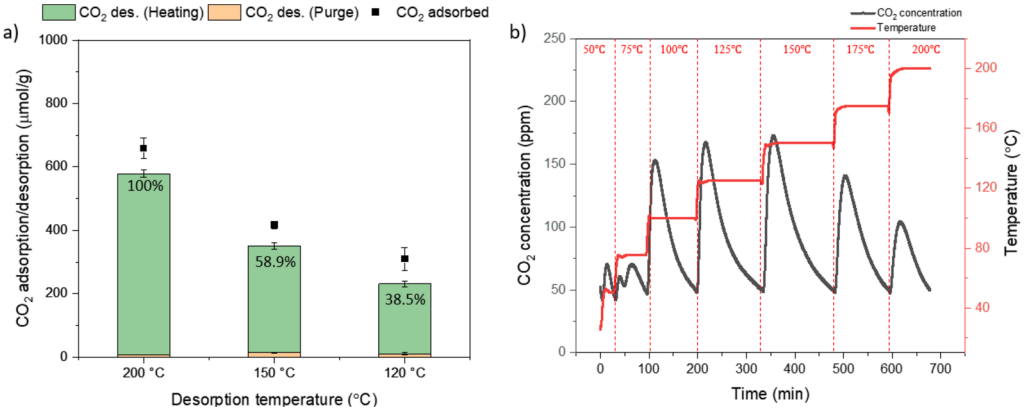

Fig. 4. A. the average adsorption and desorption performance after 5 cycles with 2.5 % Ni, 10 % "Na_2O"/Al_2O_3 under moist conditions. The adsorption capacities (20 °C, 400 ppm CO_2/air + 2 mol% H_2O) and moist desorption were conducted at each temperature. (5 °C /min, N_2 + 2 mol% H_2O). Fig. 4b. Temperature-programmed desorption profiles under moist conditions.

Table 3
The amount of CO_2 desorbed at each temperature range is reported as capacity (μ mol/g) and fraction (%) using 2.5 % Ni, 10 % "Na_2O"/Al_2O_3. All adsorptions were conducted at ambient conditions with 400 ml/min air containing 400 ppm CO_2 and 2 mol% moisture. Desorption was conducted under moist (100 ml/min N_2, 5 °C /min, 2 mol% moisture) and dry (100 ml/min N_2, 5 °C /min) conditions to the indicated temperature increment.

	Moist condition			Dry condition		
Temperature (°C)	Desorbed CO_2 (μ mol/g)	Integrated desorbed CO_2 (μ mol/g)	Fraction (%)	Desorbed CO_2 (μ mol/g)	Integrated desorbed CO_2 (μ mol/g)	Fraction (%)
25–100	160.65	160.65	28.2	90.90	90.90	27.32
100–125	124.83	285.48	21.91	27.12	118.02	8.15
125–150	122.88	408.36	21.57	43.05	161.06	12.94
150–175	84.81	493.17	14.89	71.60	232.66	21.52
175–200	76.44	569.61	13.42	100.74	333.39	30.27
Total			100			100

measured for fresh and aged samples of 2.5 % Ni with 10 % "Na_2O"/γ-Al_2O_3 at a 2θ scan range from 20° to 85° using a step size of 0.01°.

Brunauer-Emmett-Teller (BET) multi-point nitrogen adsorption was measured using ASAP 2020 Plus version 2.00 (Micromeritics, USA).

3. Result & discussion

3.1. Moisture (2 mol%) effect on CO_2 desorption with 0.25 %Ru, 10 % "Na_2O"/Al_2O_3

The viability of moist feed for adsorption and desorption in a temperature swing operation was evaluated using a sorbent sample composed of 0.25 %Ru in combination with 10 % "Na_2O"/Al_2O_3. The presence of Ru is only for the pretreatment to catalytically hydrogenate the Na_2CO_3 sorbent precursor dispersed on gamma Al_2O_3 under an H_2 flow at 350 °C. This pretreatment method generates nano-dispersed "Na_2O"/Al_2O_3 with high CO_2 capacity, as disclosed in [25] as indicated in Section 2.1.

The enhancement effect of CO_2 adsorption in moist air (2 mol%) was published previously [25] and included as black squares in Fig. 2. The addition of moisture to the feed is believed to convert nano-dispersed "Na_2O"/Al_2O_3 to nano-dispersed $2NaHCO_3/Al_2O_3$ with a high CO_2 desorption capacity of 643μ mol/g (Fig. 2, left column) relative to that in a dry inert purge gas, 503μ mol/g (right column).

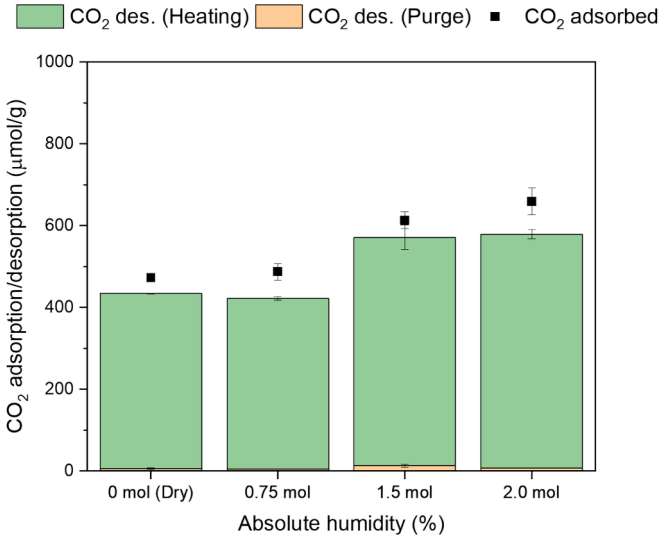

Fig. 5. The average adsorption and desorption performance (5 cycles) of 2.5 % Ni, 10 % "Na_2O"/Al_2O_3 under various moist conditions (0.75 %mol, 1.5 %mol, and 2.0 %mol). The adsorption was conducted at 20 °C with 400 ppm CO_2/air + 2 mol% H_2O. The desorption was conducted at 200 °C with 5 °C /min heating rate, and the gas used was N_2 with different moisture levels.

3.2. Replacing ruthenium with 1 % for nickel for sorbent pretreatment

Previously, we reported that Ni can replace Ru as a less expensive catalyst to hydrogenate Na_2CO_3 during pretreatment to enhance CO_2 adsorption [26]. Data in Fig. 3 reports adsorption/desorption data for a sample composed of 1 % Ni, 10 % "Na_2O"/Al_2O_3.

The CO_2 steady state adsorption (black squares) was followed by either moist desorption (left) or dry desorption (right) to 150 °C (orange) and then 200 °C (orange + green). Both moist and dry scenarios were conducted for 5 cycles. Table 1 summarizes the enhanced desorption for moist vs. dry desorption for 1 % Ni. However, Ni is less effective in catalytically decomposing the Na_2CO_3 than Ru, resulting in lower CO_2 adsorption, as seen by comparing Fig. 3 to Fig. 2. Consequently, the extent of desorption from the 1 % Ni (569 μmol/g) is lower than that of 0.25 % Ru (643 μmol/g).

3.3. Desorption using 2.5 % Ni as the catalyst for sorbent pretreatment

Fig. 4a shows the adsorption (black squares) and moist and dry desorption at three different maximum desorption temperatures using 2.5 % Ni, 10 % "Na_2O"/Al_2O_3. This sorbent replaces the Ru with 2.5 %Ni for the pretreatment to improve CO_2 enhancement. It is clearly advantageous to set a high desorption temperature to improve the yield of CO_2 but at the expense of higher energy consumption. Moist desorption performance at different temperatures (120 °C, 150 °C, and 200 °C)

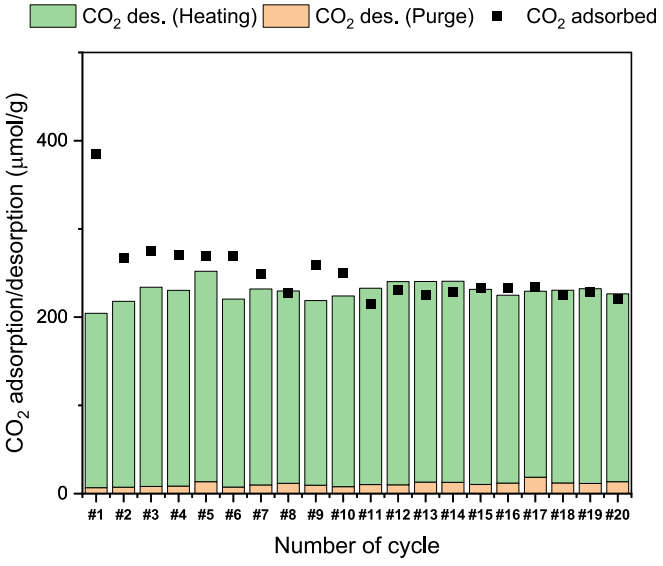

Fig. 6. Cumulative CO_2 adsorbed/desorbed during 20 cycles on 2.5 % Ni, 10 % "Na_2O"/Al_2O_3. The cyclic experiment consists of adsorption (20 °C, 400 ppm CO_2/air + 2 mol% H_2O, 3 h) and desorption (5 °C/min to 120 °C, 2 mol% H_2O in N_2) for each cycle. The adsorption and desorption are the same throughout this experiment series.

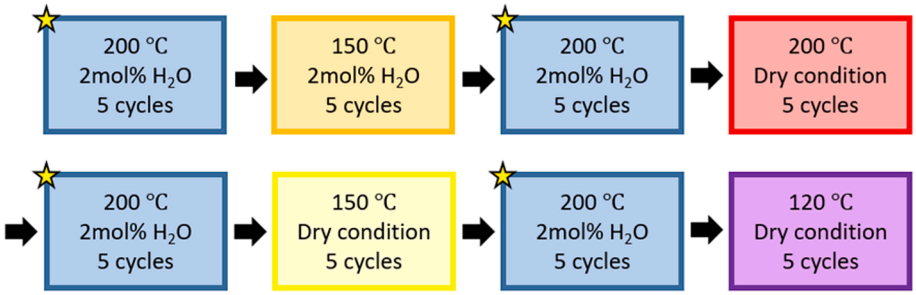

Fig. 7. The experimental aging protocol for varying desorption conditions (arrows indicate the sequence) was studied to understand performance stability. Each capture condition was conducted with 400 ppm CO_2 in air with 2 mol% moisture.

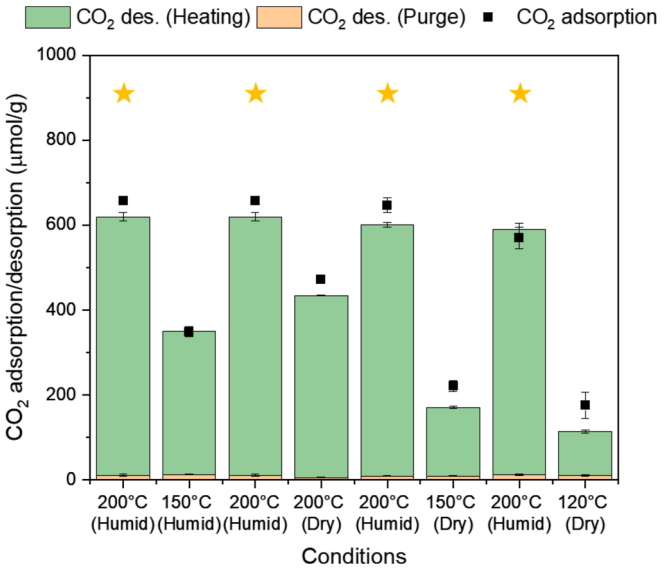

Fig. 8. Sequential cyclic performance of sample (2.5 % Ni, 10 % "Na_2O"/Al_2O_3 over time at various desorption conditions. The yellow stars highlight the stable performance at a reference condition (200 °C), after each change in desorption conditions during the cyclic tests. Cyclic tests consist of an adsorption condition of (20 °C, 400 ppm CO_2/air + 2 mol% H_2O, 3 h). Desorption conditions were (5 °C /min to target temperature, with and without 2 mol% H_2O in N_2). The error bars indicate the standard deviation for each 5-cycle test. (For interpretation of the references to colour in this figure legend, the reader is referred to the web version of this article.)

using this sample is shown in Fig. 4a.

The adsorption capacity decreases with lower desorption temperatures due to the retained CO_2 on the alkali sorbent sites. At 200 °C, nearly all CO_2 was desorbed within the error brackets shown. Using the desorption capacity at 200 °C as a reference, 58.9 % was achieved at 150 °C, and 38.5 % was achieved at 120 °C. Fig. 4b illustrates the rate of moist desorption from 25 °C to 200 °C. The amount of CO_2 in the desorption profile decreases with time because most of the adsorption capacity is sufficiently desorbed at 125 °C and 150 °C because the presence of small amount of moisture accelerates the catalytically hydrogenation of $NaHCO_3$, leading to a higher CO_2 desorption at reduced temperatures [27]. Table 2 summarizes the data at each desorption temperature.

Table 3 shows the fractions of CO_2 desorbed with and without moisture at each temperature increment. The total moist desorption capacities are lower than those of the ruthenium-containing sample (Table 2), but 2.5 % nickel is a possible replacement for more expensive ruthenium for the pretreatment, resulting in cost savings.

The rate of desorption is also faster for moist desorption than for the dry condition. On average, approximately 54 min is necessary to desorb 334 μmoles CO_2/g in the presence of moisture vs. 135 min for dry.

3.4. Desorption testing at varying moisture contents

The impact of moisture on desorption capacity was also tested on various moisture contents. Fig. 5 demonstrates the adsorption and desorption capabilities of the sample under 0.75 %, 1.5 %, and 2.0 % mol moisture levels, and the results from dry adsorption were also included as a reference point.

There is little difference in CO_2 yield between 2 mol% and 1.5 mol% moisture (572.1 μmol/g vs. 664.1 μmol/g). However, the capacity of desorption decreased to 417.7 μmol/g at 0.75 mol%, which is similar to the results of dry desorption. It is speculated that there is a threshold for the moisture enhancement effect between 0.75 mol% and 1.5 %mol. The impact of moisture is not significant in terms of desorption capacity below that threshold, while increasing the moisture doesn't significantly improve the enhanced results above that threshold. However, more investigation with other intermedium moisture levels is required for a clear conclusion.

It is better to avoid moisture levels higher than 2 mol%, which is above the vapor pressure of H_2O at the adsorption condition (20 °C). Achieving a higher moisture level requires a higher adsorption temperature, increasing energy consumption and negatively impacting adsorption capacity.

3.5. Cyclic aging for the DAC application conditions

An aging test was conducted with 2.5 % Ni, 10 % "Na_2O"/Al_2O_3 with adsorption at 20 °C followed by moist desorption (2 mol% H_2O in N_2) up to 120 °C is shown in Fig. 5. The first data point should be ignored since the surface is fresh, with no retained CO_2 from previous cycles. The data reaches a steady value after 7 or 8 cycles.

Following the tests shown in Fig. 6, the same sample (2.5 % Ni, 10 % "Na_2O"/Al_2O_3) was subjected to varying desorption conditions to establish stability according to the protocol of Fig. 7. The desorption at 200 °C under moist conditions served as the reference point (marked by a yellow star) for evaluating performance changes after 5 cycles for each desorption temperature condition. The aging performance data is presented in Fig. 8. Each capture condition was conducted with 400 ppm CO_2 in air with 2 mol% moisture added from water vapor pressure at 20 °C.

Fig. 8 provides significant data validating its desorption capacities under various sequential conditions. The results show stability after both moist and dry desorption under varied temperatures, confirming short-term system stability. This suggests that altering desorption conditions had no discernible short-term effect on the sample life.

3.6. Characterization

XRD and BET surface area measurements were made after the aging tests shown in Figs. 6 and 8. The XRD patterns in Fig. 9 show no

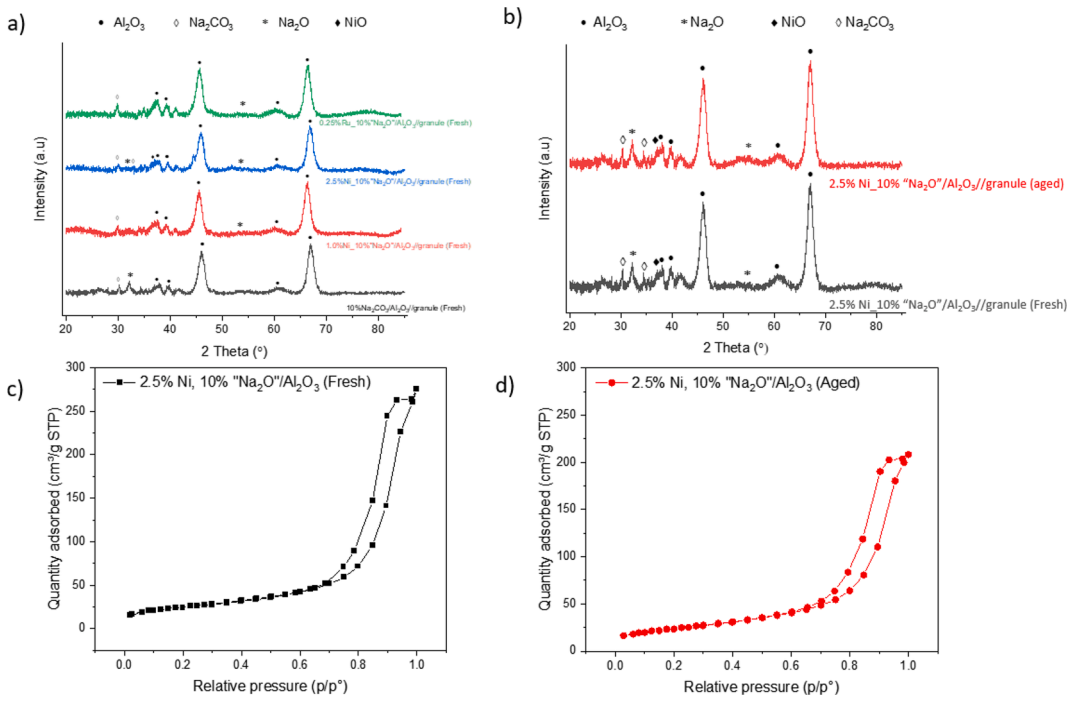

Fig. 9. a. XRD patterns for 0.25% Ru, 1.0% Ni, and 2.5% Ni with 10% "Na_2O"/Al_2O_3 for fresh sample. b. XRD patterns for fresh and aged samples (after 5 and 60 cycles) for 2.5% Ni, 10% "Na_2O"/Al_2O_3. c. Multi points of adsorption and desorption curve for fresh sample. d. for aged sample.

significant changes in the 2 θ values, peak shapes, and intensities before and after aging.

Fig. 9a shows that 0.25 % Ru, and 2.5 % Ni samples, Na_2CO_3 is only very small peak due to its catalytically hydrogenation. Furthermore, a large amount of CH_4 is observed during pretreatment of catalyst and Na_2CO_3 indicating carbonate begins to catalytically hydrogenate. Na_2O is amorphous, therefore, no peak appears because of its nano size.

Fig. 9b shows that the XRD pattern for fresh and aged 2.5 % Ni, 10 % "Na_2O"/Al_2O_3 show evidence of Al_2O_3, NiO, and traces of unreacted Na_2CO_3, consistent with our previous publication [28]. A position is shown for Na_2O [29,30]. There are minimal differences between fresh and aged samples [31]. However, between 50° and 55°, the sample showed no defined pattern for Na_2O due to its amorphous nature. A slight increase in detection is noted in the aged sample at approximately 2 θ = 54°, suggesting some minor growth in the Na_2O species. The presence of NiO is due to the oxidization of Ni after pretreatment and exposure to air during the capture step. The primary overall conclusion is that no deactivation in performance or obvious structural changes occurred during aging in the tests. Fig. 9c and 9d shows the multi points of N_2 adsorption and desorption. Both adsorption isothermal curves rapidly reached a plateau and closely followed the Langmuir isotherm model [32], but the aged sample diminished the amount of adsorbed N_2. The BET measured after the pretreatment in H_2 at 350 °C (88 m^2/g) did show some decline after aging to 86 m^2/g Nonetheless, this minor change did not affect the CO_2 desorption efficiency.

It is postulated that small amounts of moisture will enhance (i.e., catalyze) the rate of $NaHCO_3$ decomposition, producing a greater yield of CO_2 at lower temperatures compared to dry, according to the identical reactions below.

$$2NaHCO_3/Al_2O_3 \xrightarrow[\text{Dry}]{} Na_2O/Al_2O_3 + 2CO_2 + H_2O \quad \text{(slow reaction at elevated temperature)}$$

$$2NaHCO_3/Al_2O_3 \xrightarrow[\text{Moisture}]{} Na_2O/Al_2O_3 + 2CO_2 + H_2O \quad \text{(fast reaction at low temperature)}$$

4. Conclusion

A sorbent system composed of 2.5 % Ni, 10 % "Na_2O"/Al_2O_3 provides an improvement in direct air capture for both CO_2 adsorption and moist desorption. The presence of 2 mol % moisture, which was generated at the vapor pressure of water at 20 °C for desorption, enhances the yield of CO_2 at lower temperatures and a higher rate relative to a dry desorption purge. The low partial pressure of moisture avoids the necessity to generate steam and its energy penalty. A 60-cycle aging study (317 h) was conducted at varying maximum desorption temperatures (120 °C, 150 °C, 200 °C). The test protocol included both moist and dry desorption conditions, with results showing initial stability of the material as consistent with XRD results.

The preliminary laboratory-scale study underscores the technical value of low energy content moisture in decomposing nano-dispersed $NaHCO_3/Al_2O_3$ with the liberation of larger yields of CO_2 than for the dry purge.

CRediT authorship contribution statement

Soosan Kim: Writing – review & editing, Writing – original draft, Visualization, Resources, Project administration, Methodology, Investigation, Formal analysis, Data curation, Conceptualization. **Xiao Lin:** Writing – review & editing, Formal analysis. **Robert J. Farrauto:** Writing – review & editing, Supervision, Conceptualization.

Declaration of competing interest

The authors declare that they have no known competing financial interests or personal relationships that could have appeared to influence the work reported in this paper.

Data availability

Data will be made available on request.

Acknowledgments

The authors would like to acknowledge Ms. Vicki Gould and the J.G. Cohn Memorial Fellowship for many years of support in environmental catalysis research. We also want to thank Sasol, Anglo American, and NGK Insulators for providing materials and insights.

References

[1] P. Panja, C. Manankandayalage, M.M. Alam, M. Deo, Understanding the performance of membrane for direct air capture of CO2, J. Appl. Polym. Sci. 141 (3) (2024) e54802.
[2] K. Yuan, T. Zhang, X. Xie, S. Du, X. Xue, A.F. Abdul-Manan, Z. Huang, Exploration of low-cost green transition opportunities for China's power system under dual carbon goals, J. Clean. Prod. 414 (2023) 137590.
[3] G. Li, X. Shen, X. Jiao, F. Xie, J. Hua, H. Lin, F. Yan, H. Wu, Z. Zhang, Novel tri-solvent amines absorption for flue gas CO2 capture: Efficient absorption and regeneration with low energy consumption, Chem. Eng. J. 152699 (2024).
[4] R. Hunt, J. Gillbanks, J. Czapla, Z. Wan, C. Karmelich, C. White, C. Wood, Representative longevity testing of direct air capture materials, Chem. Eng. J. 481 (2024) 148901.
[5] S.R. Wenger, D.M. D'Alessandro, Improving the sustainability of electrochemical direct air capture in a 3D printed redox flow cell, ACS Sustain. Chem. Eng. (2024).
[6] V. Gama, B. Dantas, O. Sanyal, F.V. Lima, Process operability analysis of membrane-based direct air capture for low-purity CO2 production, ACS Eng. Au (2024).
[7] H.E. Holmes, M.J. Realff, R.P. Lively, Water management and heat integration in direct air capture systems, Nat. Chem. Eng. (2024) 1–8.
[8] M.J.B. Kabeyi, O.A. Olanrewaju, Carbon Capture and Sequestration and Carbon Capture and Use.
[9] F. Bisotti, K.A. Hoff, A. Mathisen, J. Hovland, Direct Air capture (DAC) deployment: A review of the industrial deployment, Chem. Eng. Sci. 283 (2024) 119416.
[10] E.C. Okonkwo, A. AlNouss, M. Shahbaz, T. Al-Ansari, Developing integrated direct air capture and bioenergy with carbon capture and storage systems: progress towards 2° C and 1.5° C climate goals, Energ. Conver. Manage. 296 (2023) 117687.
[11] B.R. Roger, Process for separating acidic gases, United State (1933) 5.
[12] F. Meng, Y. Meng, T. Ju, S. Han, L. Lin, J. Jiang, Research progress of aqueous amine solution for CO2 capture: A review, Renew. Sustain. Energy Rev. 168 (2022) 112902.
[13] B.M. Balasubramaniam, P.-T. Thierry, S. Lethier, V. Pugnet, P. Llewellyn, A. Rajendran, Process-performance of solid sorbents for Direct Air Capture (DAC) of CO2 in optimized temperature-vacuum swing adsorption (TVSA) cycles, Chem. Eng. J. 485 (2024) 149568.
[14] Z. Tan, S. Zhang, F. Zhao, R. Zhang, F. Tang, K. You, H.a. Luo, X. Zhang, SnO2/ATP catalyst enabling energy-efficient and green amine-based CO2 capture, Chem. Eng. J. 453 (2023) 139801.
[15] R. Hanna, A. Abdulla, Y. Xu, D.G. Victor, Emergency deployment of direct air capture as a response to the climate crisis, Nat. Commun. 12 (1) (2021) 368.
[16] M. Ozkan, Atmospheric alchemy: The energy and cost dynamics of direct air carbon capture, MRS Energy Sustainab. (2024) 1–16.
[17] X. Duan, G. Song, G. Lu, Y. Wang, J. Sun, A. Chen, X. Xie, Chemisorption and regeneration of amine-based CO2 sorbents in direct air capture, Mater. Today Sustainab. 23 (2023) 100453.
[18] J.S. Carneiro, G. Innocenti, H.J. Moon, Y. Guta, L. Proaño, C. Sievers, M.A. Sakwa-Novak, E.W. Ping, C.W. Jones, Insights into the Oxidative degradation mechanism of solid amine sorbents for CO2 capture from air: roles of atmospheric water, Angew. Chem. 135 (24) (2023) e202302887.
[19] R. Rodríguez-Mosqueda, E.A. Bramer, G. Brem, CO2 capture from ambient air using hydrated Na2CO3 supported on activated carbon honeycombs with application to CO2 enrichment in greenhouses, Chem. Eng. Sci. 189 (2018) 114–122.
[20] L. Proaño, E. Tello, M.A. Arellano-Trevino, S. Wang, R.J. Farrauto, M. Cobo, In-situ DRIFTS study of two-step CO2 capture and catalytic methanation over Ru, "Na2O"/Al2O3 Dual Functional Material, Appl. Surf. Sci. 479 (2019) 25–30.
[21] M. Goldman, S. Kota, X. Gao, L. Katzman, R. Farrauto, Parametric and laboratory aging studies of direct CO2 air capture simulating ambient capture conditions and desorption of CO2 on supported alkaline adsorbents, Carbon Capture Science & Technology 6 (2023) 100094.
[22] M.J. Abdallah, J.E. Peters, T. Luo, H. Sheng, Y.L. Chen, R.J. Farrauto, Aging studies of Dual functional materials for CO2 direct air capture with in situ methanation under simulated ambient conditions: Ru thrifting for cost reduction, Chem. Eng. J. 479 (2024) 147495.
[23] M. Abdallah, R. Farrauto, Laboratory aging of a dual function material (DFM) washcoated monolith for varying ambient direct air capture of CO2 and in situ catalytic conversion to CH4, Appl Catal B 339 (2023) 123105.
[24] C. Jeong-Potter, A. Porta, R. Matarrese, C.G. Visconti, L. Lietti, R. Farrauto, Aging study of low Ru loading dual function materials (DFM) for combined power plant effluent CO2 capture and methanation, Appl. Catal. B 310 (2022) 121294.
[25] M. Abdallah, R. Farrauto, A perspective on bridging academic research and advanced testing on a path towards pilot plant implementation: A case study of integrating CO2 capture and catalytic conversion with dual function materials, Catal. Today 423 (2023) 113923.
[26] C. Jeong-Potter, M. Abdallah, S. Kota, R. Farrauto, Enhancing the CO2 adsorption capacity of γ-Al2O3 supported alkali and alkaline-earth metals: impacts of dual function material (DFM) preparation methods, Ind. Eng. Chem. Res. 61 (29) (2022) 10474–10482.
[27] W.-Y. Kuu, R. Chilamkurti, C. Chen, Effect of relative humidity and temperature on moisture sorption and stability of sodium bicarbonate powder, Int. J. Pharm. 166 (2) (1998) 167–175.
[28] S. Wang, R.J. Farrauto, S. Karp, J.H. Jeon, E.T. Schrunk, Parametric, cyclic aging and characterization studies for CO2 capture from flue gas and catalytic conversion to synthetic natural gas using a dual functional material (DFM), J. CO2 Util. 27 (2018) 390–397.
[29] R. Prins, On the structure of γ-Al2O3, J. Catal. 392 (2020) 336–346.
[30] L. He, Y. Ren, B. Yue, S.C.E. Tsang, H. He, Tuning metal–support interactions on Ni/Al2O3 catalysts to improve catalytic activity and stability for dry reforming of methane, Processes 9 (4) (2021) 706.
[31] C. Jeong-Potter, A. Zangiabadi, R. Farrauto, Extended aging of Ru-Ni, Na2O/Al2O3 dual function materials (DFM) for combined capture and subsequent catalytic methanation of CO2 from power plant flue gas, Fuel 328 (2022) 125283.
[32] Y.-J. Lee, Y.J. Jeong, I.S. Cho, C.-G. Lee, S.-J. Park, P.J. Alvarez, The inhibitory mechanism of humic acids on photocatalytic generation of reactive oxygen species by TiO2 depends on the crystalline phase, Chem. Eng. J. 476 (2023) 146785.